SUPPLEMENTAL MATERIAL

THE EFFECT OF LAYER-BY-LAYER BUILDING IN SELECTIVE LASER SINTERING ON THE PERFORMANCE OF POLYMER-BASED THz OPTICAL SYSTEMS

Gabriel MOAGĂR-POLADIAN[(*)(1)], Cătălin TIBEICĂ[(1)]
[(1)] *National Institute for Research and Development in Microtechnology – IMT Bucharest*
Str. Erou Iancu Nicolae 126A, 077190, Bucureşti-Voluntari, ROMANIA
[(*)] *E-mail: gabriel.moagar@imt.ro*

In this Annex we present the detailed simulations of the lenses.

We compare how a 3D-printed, stepwise lens behaves with respect to a perfect (smooth) lens in figures S1-S4. The focal plane was considered at the distance where the electric field reaches its maximum for a normal, θ = 0º incident wavefront.

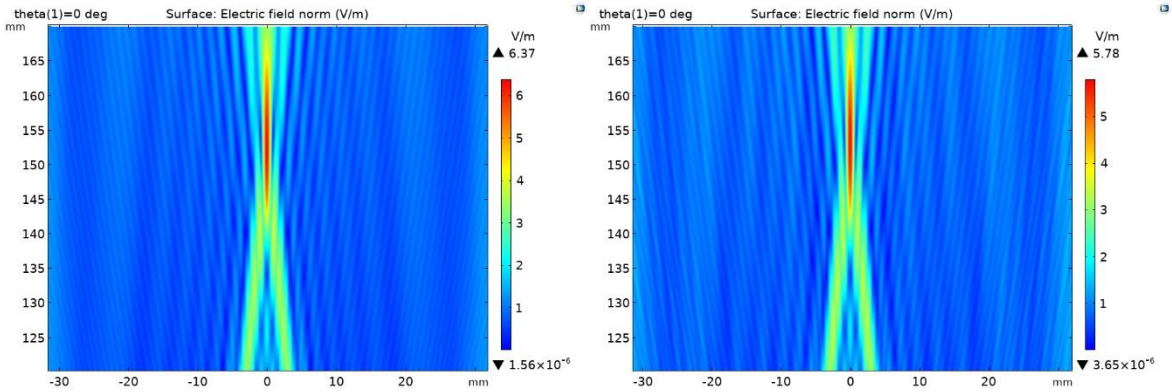

Figure S1 - Electric field (normE) in focal region, at normal incidence (θ = 0º) of the incident plane wavefront. Left - smooth (perfect) lens; Right - stepwise (printed) lens.

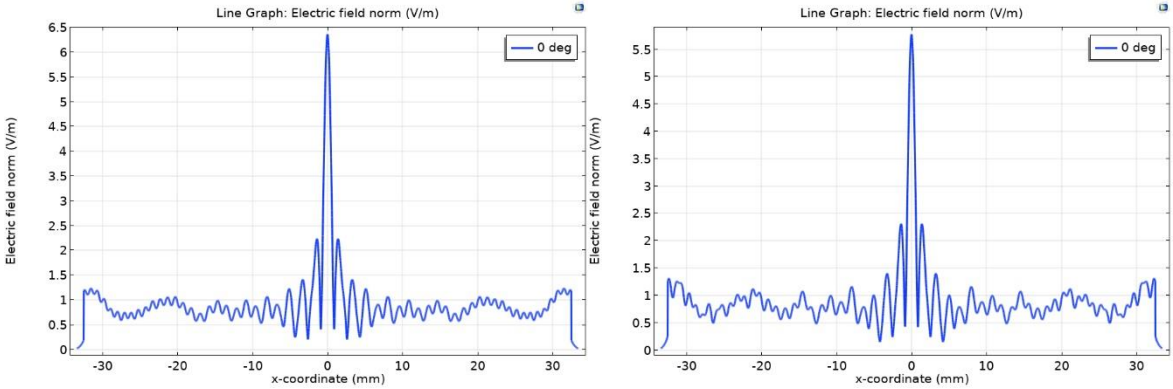

Figure S2 - Electric field distribution in the focal plane (cross section normal to the propagation direction), at normal incidence (θ = 0º). Left - smooth (perfect) lens; Right - stepwise (printed) lens.

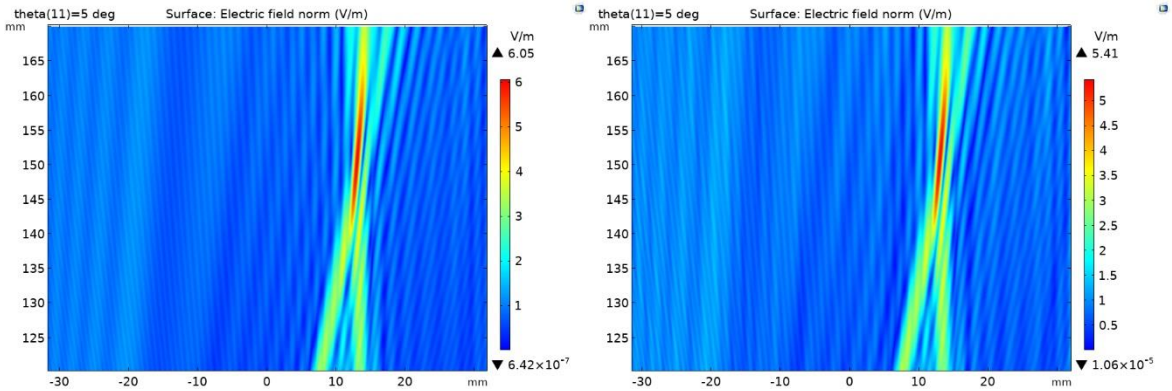

Figure S3 - Electric field (normE) in focal region, at oblique incidence (θ = 5º) of the incident plane wavefront. Left - smooth (perfect) lens; Right - stepwise (printed) lens.

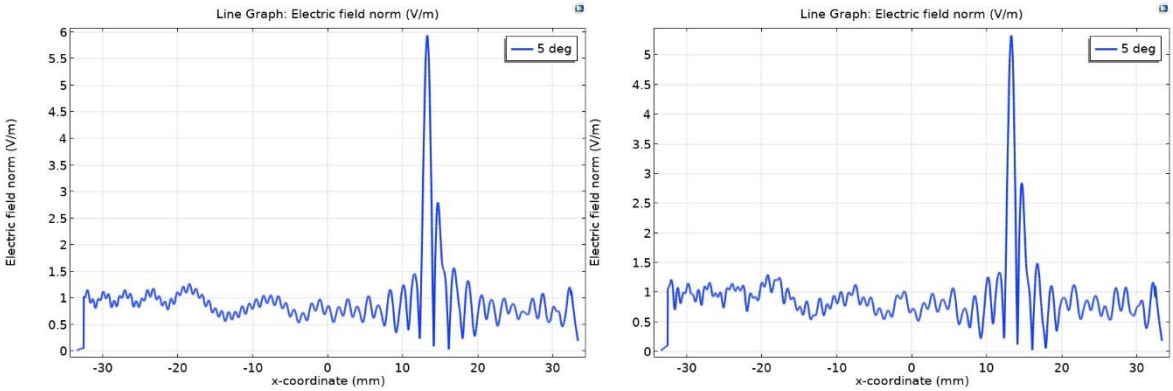

Figure S4 - Electric field distribution in the focal plane, at oblique incidence (θ = 5º). Left - smooth (perfect) lens; Right - stepwise (printed) lens.

As can be noticed from figures S1-S4, the differences between the two lenses are very small and allow us to state that the stepwise lens performs practically similar to the smooth surface one. This happens because diffraction on the steps and edges resulted from the AM process "tames" the respective geometrical irregularities.

A.2 Stepwise lens at three different wavelengths

In this case, we consider a SLS-made plano-convex spherical lens with the parameters: Lens diameter, D_{Lens} = 40 mm; Lens sagitta, s_{Lens} = 5 mm; Lens thickness, t_{Lens} = 10 mm. The print layer height is Δz = 0.1 mm. The refractive index is n_{Lens} = 1.516 and is the same at the two wavelengths considered: λ_1 = 3 mm, λ_2 = 0.3 mm, λ_3 = 0.2 mm (in air), corresponding to frequencies ν_1 = 100 GHz, ν_2 = 1 THz, ν_3 = 1.5 THz.

The discretization step is $N_{Mesh} = \lambda/8$. Simulations were performed considering an incoming plane wave of 1 V/m amplitude at normal incidence.

Figure S5 depicts the electric field amplitude at the three frequencies. Figure S6 displays the electric field value in the focal plane (normal to the propagation direction).

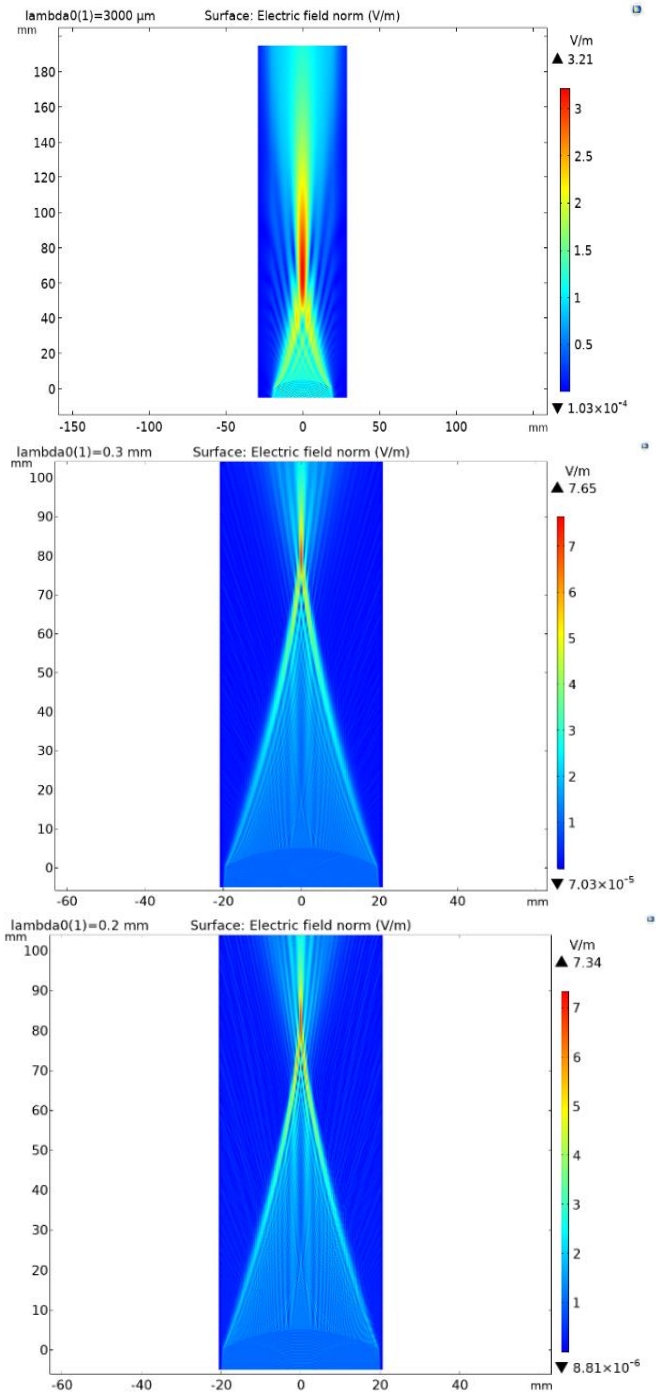

Figure S5 - Electric field distribution in the focused beam. Top: at 100 GHz; Centre: at 1 THz; Bottom: at 1.5 THz.

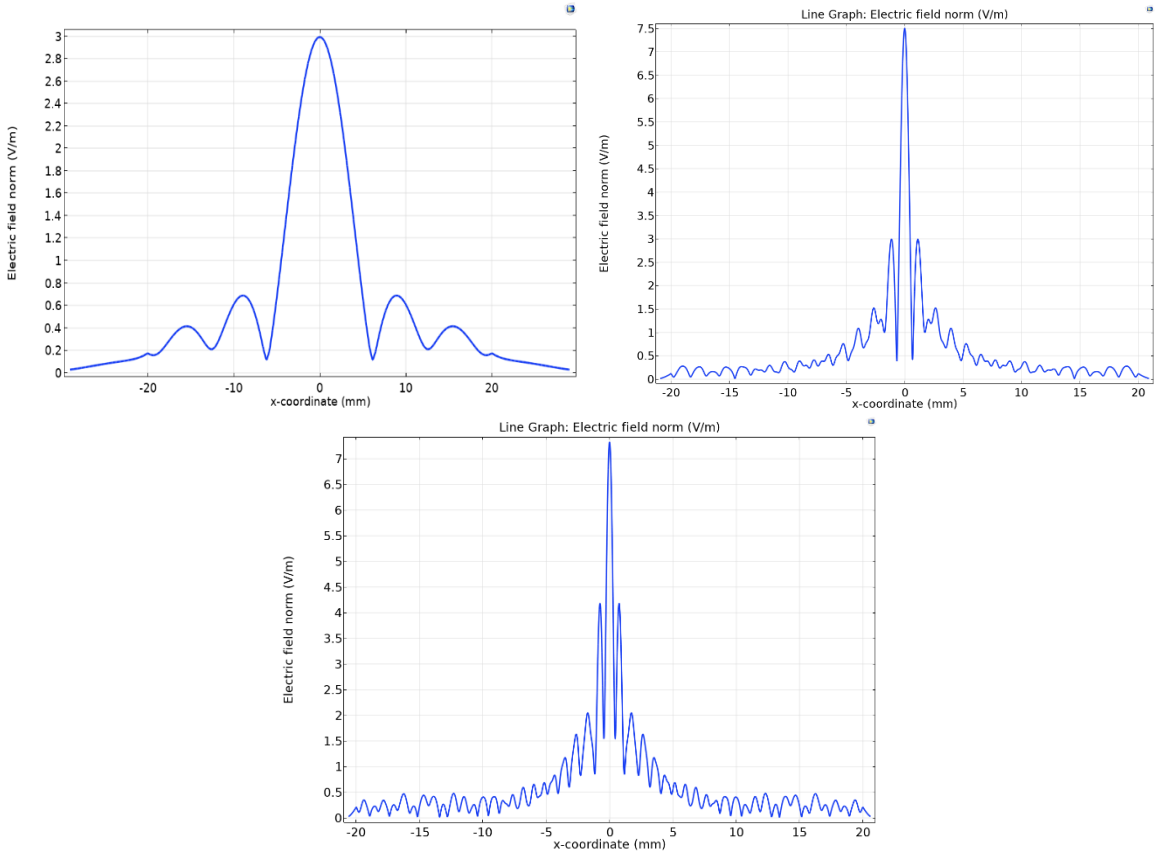

Figure S6 - Electric field distribution in the focal plane. Top left: at 100 GHz; Top right: at 1 THz; Bottom centre: at 1.5 THz.

It is noticed from figure S6 that the electric field distribution is smoother for the 1THz radiation than for 1.5 THz. This happens because diffraction plays a crucial role in smoothening the spatial distribution of the electric field at lower frequencies (longer wavelengths).

A.3 Image of a point-like source

The simulation parameters are:

D_{lens} = 50 mm,

s_{lens} = 4 mm,

t_{lens} = 8 mm

Object plane – lens distance, y1 = 459.5 mm

Lens – image plane distance, y2 = 228 mm

Refractive index, n_{Lens} = 1.516

Wavelength = 0.3 mm (in air), frequency 1 THz

The field distribution immediately after the pinhole is shown in figure S7 while figure S.8 depicts the point image formation for the stepwise lens for the two positions (optical axis, and displaced at 10 mm, respectively).

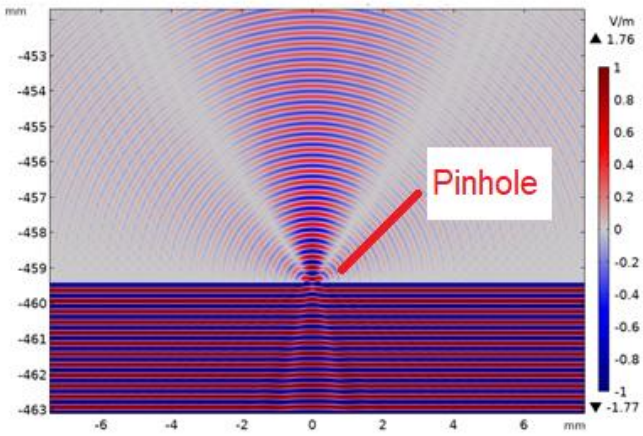

Figure S.7 - Electric field amplitude through the pinhole.

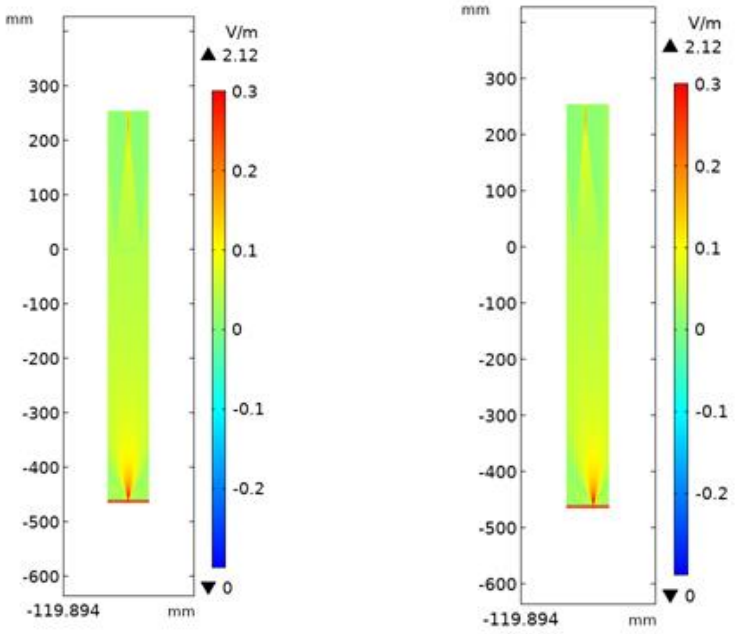

Figure S.8 - Point image formation for the stepwise lens. Left: point object on the optical axis; Right: point object radially displaced at 10 mm from the optical axis.

It is observed from figure S.8 that the point object is focused to a point image for each of the object's positions.

A.4 Image of a distribution of point-like sources

The distribution of the field amplitude of the waves emanating from the point sources are depicted in figure S.9, where characteristic interference fringes are clearly visible.

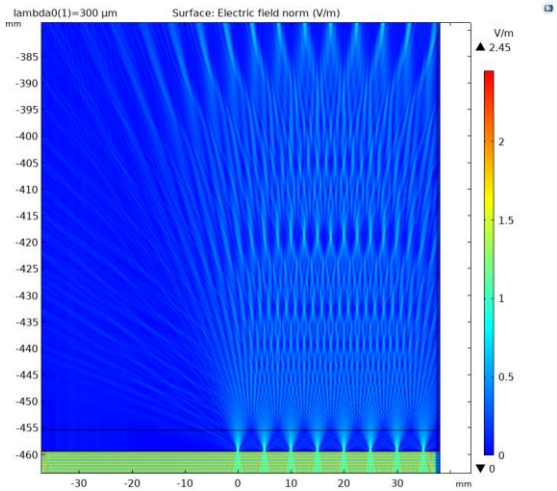

Figure S.9 – The distribution of the field amplitude of the waves emanating from the point sources.

Figure S.10 depicts the electric field map and the radial distribution of the electric field in the image plane, respectively. As expected, each of the lenses performs image inversion (i.e., the image is inverted with respect to the object). The radial distribution shows good similarity between the two lenses.

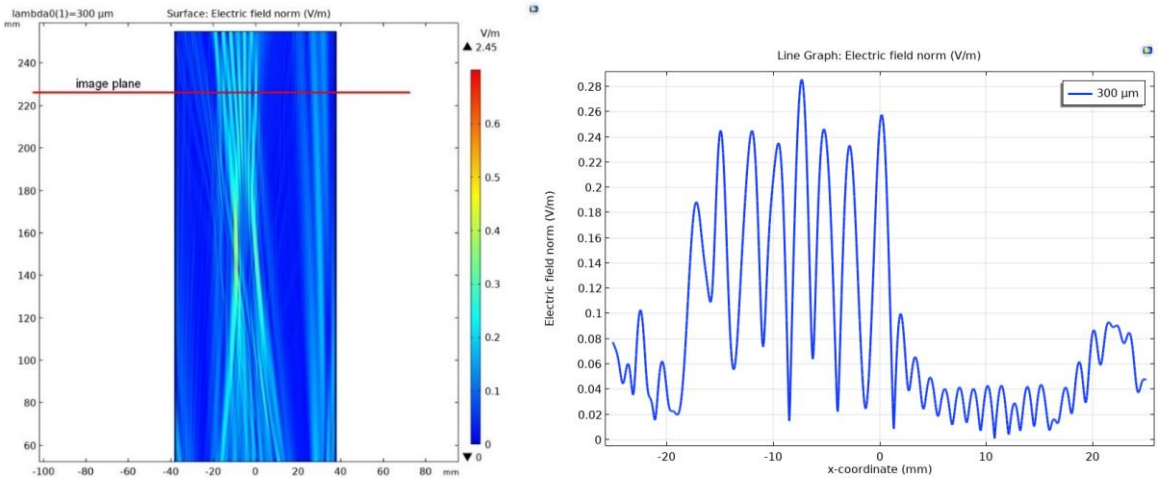

a)

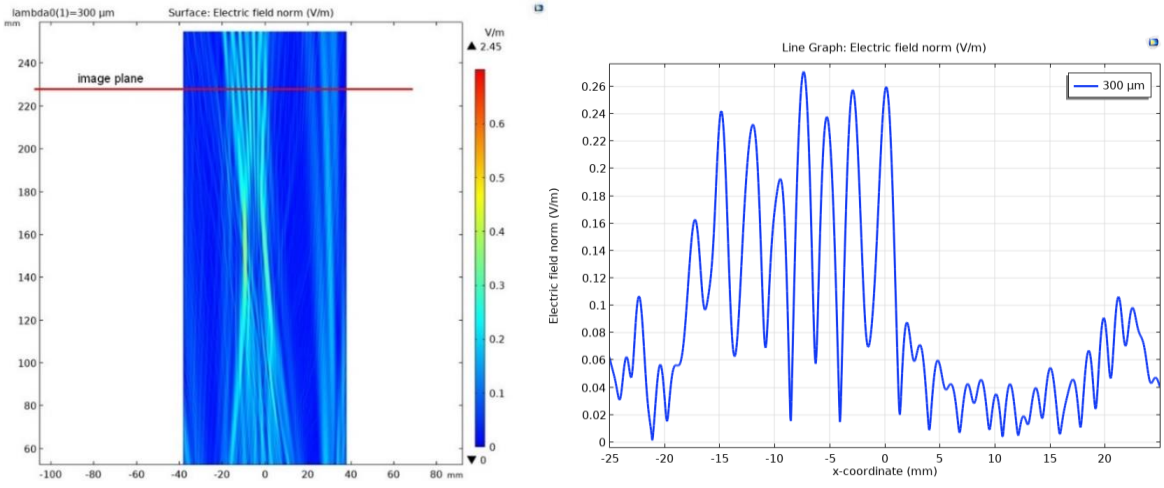

b)

Figure S.10 – The electric field map (left) and radial distribution of the electric field (right) in the image plane. a) smooth lens; b) stepwise lens.